

## Status of the DARHT Phase 2 Long-Pulse Accelerator\*

M.J. Burns, B.E. Carlsten, H.A. Davis, C.A. Ekdahl, C.M. Fortgang, B.T. McCuistian, F.E. Merrill,  
K.E. Nielsen, C.A. Wilkinson  
Los Alamos National Laboratory, P.O Box 1663, Los Alamos, NM 87544

K.P. Chow, W.M. Fawley, H.L. Rutkowski, W.L. Waldron, S.S. Yu  
E.O. Lawrence Berkeley National Laboratory, 1 Cyclotron Rd., Berkeley, CA 94720

G.J. Caporaso, Y.-J. Chen, E.G. Cook, S. Sampayan, J.A. Watson, G.A. Westenskow  
Lawrence Livermore National Laboratory, 7000 East Ave., Livermore, CA 94550

T.P. Hughes

Mission Research Corporation, 5001 Indian School Rd., Albuquerque, NM 87110

### Abstract

The Dual-Axis Radiographic Hydrodynamics Test (DARHT) facility will employ two perpendicular electron Linear Induction Accelerators to produce intense, bremsstrahlung x-ray pulses for flash radiography. We intend to produce measurements containing three-dimensional information with sub-millimeter spatial resolution of the interior features of very dense, explosively-driven objects. The facility will be completed in two phases with the first phase having become operational in July 1999 utilizing a single-pulse, 20-MeV, 2 -kA, 60-ns accelerator, a high-resolution electro-optical x-ray imaging system, and other hydrodynamics testing systems. The second phase will be operational in 2004 and features the addition of a 20-MeV, 2-kA, 2-microsecond accelerator. Four short electron micropulses of variable pulse-width and spacing will be chopped out of the original, long accelerator pulse for producing time-resolved x-ray images. The second phase also features an extended, high-resolution electro-optical x-ray system with a framing speed of 1.6-MHz. Production of the first beam from the Phase 2 injector will occur this year. In this paper we will present the overall design of the Phase 2 long-pulse injector and accelerator as well as some component test results. We will also discuss the downstream transport section that contains the fast kicker used to separate the long-pulse beam into short bursts suitable for radiography as well as the x-ray conversion target assembly. Selected experimental results from this area of the project will also be included. Finally, we will discuss our plans for initial operations.

### 1. INTRODUCTION

Maintenance of a smaller, aging U.S. nuclear weapons stockpile without underground nuclear testing (UGT) requires the capability to verify and benchmark the complex computer calculations on which stockpile

confidence will be based. A key to this capability will be evaluation of the primaries of U.S. nuclear weapons through non-nuclear hydrodynamic testing, or "hydrotesting". These tests utilize very powerful x-ray sources to radiograph a full-scale, non-nuclear mock-up of a nuclear weapon primary during the late stages of the implosion, returning data on shapes, densities, and edge locations. (In the future, other probes such as tens-of-GeV-energy proton beams may also be used.) DARHT will be the first U.S. hydrotesting facility in the post-



Fig. 1 Aerial view of the DARHT facility. The 2-microsecond pulse-width second accelerator is now being installed in the portion of the building running from left to right.

UGT era and will address evolving DOE requirements by developing images with sub-millimeter resolution, from two views (the minimum for large-scale three-dimensional information), and with multiple views along one axis.

Each leg of DARHT is a x-ray imaging system. Two simultaneous images from perpendicular directions are the minimum required for 3D data and thus the essential layout of the facility is determined. To generate X-rays, we tightly focus the electron beam from the accelerator onto a high-Z x-ray conversion target. X-rays are attenuated through the object that has been explosively compressed at velocities of many km/sec. A ~250,000 element segmented scintillator converts x-rays to light, which is lens-coupled onto a mosaic of large-area charge-coupled devices (CCD).

\* Work supported by the U.S. Department of Energy under contracts W-7405-Eng-36 (LANL), DE-AC03-76SF00098 (LBNL), and W-7405-Eng-48 (LLNL).

An information theory based Figure-of-Merit (FOM) has been developed [1] to help design systems such as DARHT. The FOM is developed as the product of the system blur (characterized by the MTF [2], or area under the Modulation Transfer Function curve for the system) and the amplitude signal-to-noise ratio (SNR). The MTF is inversely proportional to the three principal blurs (source blur, detector blur, and object motion blur) added in quadrature. The SNR is proportional to the square root of the product of the x-ray dose 1-m from the conversion target, the number of photons per square-mm per R @ 1-m (a function of the electron beam energy), the x-ray transmission of the object, and the detective quantum efficiency of the detection system.

X-ray scatter limits the resolution of dense-object images using MeV-radiography. Generally, x-ray scatter causes a background noise in the image and has been partially mitigated by "graded collimation" (being thick where the object is thin and thin where the object is thick. This helps to control scatter and also reduces the dynamic ranger required in the detector). Proper electron beam energy selection has been required to best match the bremsstrahlung spectrum with the objects of interest. We find an optimum electron beam energy between 12-20 MeV that balances photoelectric absorption and Thompson scattering (the predominant scatter mechanisms at low energy) with Compton scattering and pair production (more important at high energies). X-ray dose is almost a cubic power of the beam energy and therefore we pick the highest energy practicable with respect to scatter, or 20-MeV.

A short pulse-width is needed to reduce motion blur. At a given electron energy, high peak currents are then required to generate sufficient x-ray dose (dose being proportional to the total charge striking the conversion target). We selected a Linear Induction Accelerator (LIA) to provide the required high dose at moderate energy with short pulse length. A preoccupation with dose is not warranted because the spot blurs and detector blurs are dominant. Therefore, the design of the DARHT accelerators is driven most by the need to generate a small spot size and with a sensitive detector design of high cut-off frequency.

The first axis of DARHT utilizes a well-engineered conventional LIA to produce a single high-resolution x-ray image. With the second axis of DARHT, hydrotesting needs required us to produce four high-quality images over a time-span of 2-microseconds. We address this design with a 2-microsec. pulse-width LIA whose output is chopped into four pulses of variable pulse-width and spacing. The parameters of the operating first axis of DARHT and the design parameters of the second axis system are shown in Table. 1

This paper is concerned with the accelerator driving the second axis of DARHT. This machine is a collaboration between LANL, LBNL, and LLNL. It starts with a large Marx-driven injector utilizing a hot cathode and immediate

post-acceleration. The injector rise-time is shortened in the Beam Clean-Up Zone (BCUZ) and the beam driven to its final energy through an accelerator consisting of identical LIA modules driven by individual PFNs. The transport region of the machine consists of the Kicker

<i>Parameter</i>	<i>First Axis</i>	<i>Second Axis</i>
Spot size (mm)	2.0 @ 50% MTF	≤ 2.1
Dose (R@1m)	500	variable
Pulse width (ns)	60	variable
DQE (%)	≥30	≥40
F <sub>c</sub> (cycles/mm)	≥0.3 (-3dB)	≥0.3 (-3dB)
Pixel Size (mm)	0.9 x 0.9	1 x 1
1st conjugate (m)	0.8 to 1.5	1.1
Magnification	≤ 4	≤ 4
<i>Accelerator Parameters</i>		
Energy (MeV)	19.8	18.4
Current (kA)	2	2
Pulse width (ns)	60	2000
Energy spread	< ± 1%	< ± 1%
Norm. emittance (4-rms, πcm-rad)	0.15	0.15
Grad. (MeV/m)	0.47	0.35

system that chops the beam into short micropulses useful for radiography, transport magnets, and the 4-pulse x-ray conversion target system. A layout of the machine is shown in Fig. 2.

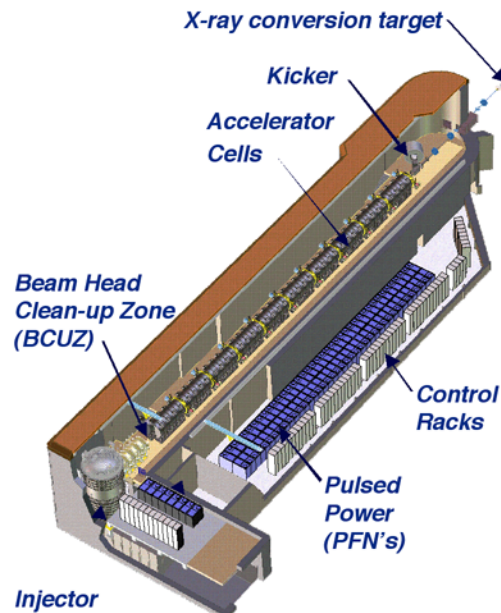


Fig. 2. Layout of the 2-microsecond pulse-width DARHT second axis accelerator system

We will present this machine by first describing in Section 2 the injector and its associated accelerator section and BCUZ. In Section 3 we will discuss the accelerator and its pulsed power. In Section 4 the Kicker will be

presented. Section 5 briefly discusses the x-ray conversion target system. We close in Section 6 with a very brief overview of our plans for initial operation.

## 2. INJECTOR

Space restrictions within the existing DARHT facility forced the injector to occupy two levels. On the bottom level is the Marx prime power feeding a vertical insulating column that drives a flat, 165-mm dia. dispenser-cathode with polished stainless steel electrodes. The Marx consists of 88 type E PFN stages driving a matched load at 3.2-MV with a nominal 500-ns rise, 2- $\mu$ s flat pulse. A triggered crowbar switch is used to shorten the pulse tail. The 444.5-cm tall, oil-filled insulator column has both alumina and Mycalex insulating rings. The peak electric field stress on the cathode shroud is 120-kV/cm with 2-kA beam current. The design beam emittance (norm,4-rms) is 0.05- $\pi$ cm-rad. A layout of the injector is shown in Fig. 3.

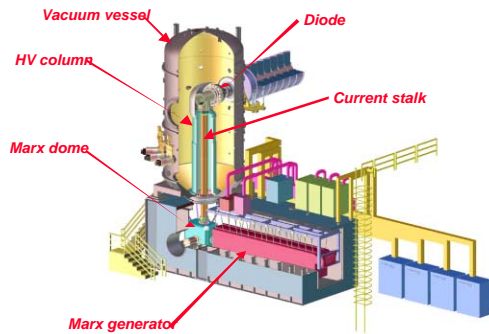


Fig. 3 Injector layout. Note stairway at extreme left for scale

Extensive testing of the Marx prime power into a dummy load was conducted prior to shipment of the unit to Los Alamos. Fig. 4 shows a typical waveform at the nominal operating voltage with the use of the crowbar switch to shorten the pulse tail. This pulse is flat to within  $\pm 1\%$  for 2-microseconds.

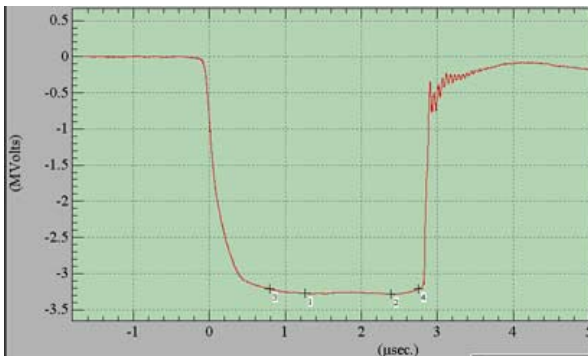


Fig. 4 2- $\mu$ s injector pulse into a dummy load is flat to within  $\pm 1\%$  with a crowbar switch used to shorten the pulse tail

We have built a Cathode Test Stand (CTS) to investigate engineering and physics issues regarding the

large (165-mm dia.) thermionic dispenser cathode. The cathode operates at 1100 °C and requires about 3 kW of heater power. We have used the CTS to investigate thermal issues, temperature uniformity, and emitted current uniformity. Our initial temperature uniformity measurements observed a non-axisymmetric cold spot attributable to the heater design [3]. Cathode redesign has mitigated this issue and on the CTS we have achieved fully space-charge limited emission at a current density of 9.4 A/cm<sup>2</sup> at 1076 °C (Fig. 5). Emission uniformity meets our requirements, showing <5% variation. The emission measurements used a unique diagnostic to measure current emission directly off the cathode surface. Because the perveance of this diagnostic is extremely high ( $\sim 400 \mu$ P) we can extract DARHT relevant current densities (10 A/cm<sup>2</sup>) at a modest operating voltage of 20 kV (as opposed to 3.2 MV on the injector).

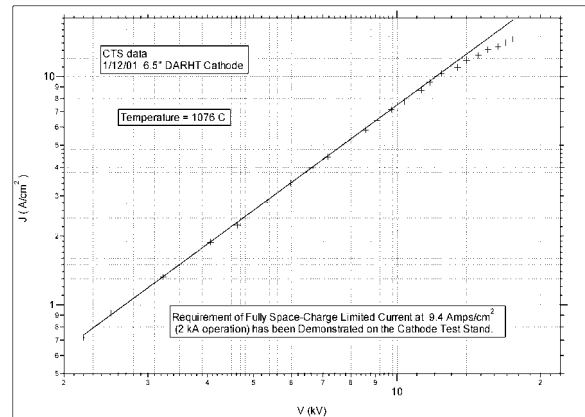


Fig. 5 CTS results showing space-charge limited

The risetime of the injector current pulse is about 500-ns and as a result there is a considerable amount of beam charge that is mismatched to the solenoid magnetic transport of the accelerator. To avoid the possibility of breakdown in the accelerator resulting from the loss of this charge, we accelerate the beam to 4.5-MeV through eight induction cells with an accelerating potential of 0.17MV and a bore of 356-mm. We then eliminate most of the beam head in the Beam Clean-Up Zone (BCUZ) that consists of a section of beam-pipe about 3-m long, three solenoids, and two apertures, each 152-mm in diameter. Extensive numerical modeling [4] indicates the beam head is successfully controlled by this approach.

## 3. ACCELERATOR & PULSE POWER

Eight induction cells immediately follow the injector diode with a 356-mm dia. beam pipe and a 173-kV accelerating potential. Matching from the injector into these cells is done with wire-wound solenoid magnets within the injector diode and the first cells. After the BCUZ, the remaining 70 induction cells have a 254-mm dia. pipe and supply 197-kV. The larger bore cells intercept essentially no beam from the injector rise time and reduce transverse impedance in a region susceptible to

BBU because of the low transport field. All of the oil insulated cells use 4 individual cores of Allied Signal 2605SC Metglas with either 0.48 V-sec core capacity or 0.43 V-sec in the large bore cells. A 200-ns rise-time leads to a 2.02- $\mu$ s flattop. A Mycalex conical insulator is used in each cell is for its excellent breakdown and mechanical properties. Each individually mounted cell contains a transport solenoid and a steering coil. Ferrite damping is employed to reduce the cell quality factor. Fig. 6 shows the eight injector induction cells during installation.



Fig. 6 The large bore induction cells during installation immediately downstream of the injector

Each induction cell has an individual cell-driver which contains 4, 7-section E-network PFNs in a Marx configuration. Each driver has a 20- $\Omega$  impedance and will deliver a 2.4- $\mu$ s flattop into a resistive load of 5- $\Omega$  for a total drive current of 10-kA at 200kV. To compensate for the non-linear magnetization current of the Metglass cores, the PFN impedance varies from front to back. The impedance of each PFN can also be reduced 20% to tune for a  $\pm 0.5\%$  flattop.

#### 4. KICKER

The principal element of the beam transport section is the fast deflector, or kicker system [5], used to generate four micropulses from the primary accelerator beam. It is similar in design to stripline beam position monitors. There are four equal size electrodes enclosed within a vacuum housing that has a DC bias magnetic dipole wound over the enclosure. An opposite pair of electrodes is driven by a fast amplifier through transit time isolated 50- $\Omega$  cables to provide beam deflection. The other two electrodes are terminated at their 50- $\Omega$  matched impedance. A subsequent drift space of several meters allows a substantial relative deflection to develop between the output beam positions of the kicker and drift. A DC septum magnet allows the separation of the two output beams. The bias dipole will deflect the beam off-axis into a large-bore, weak quadrupole magnet septum beam pipe. This magnet deflects the off-axis beam into a strong dipole magnet that transports the beam into a dump. When an x-ray pulse is desired the kicker pulsers are

activated and overcome the bias field allowing a short segment of beam to travel down the axis through the null field region of the quadrupole magnet and on to the x-ray converter target. Fig. 7 shows the Kicker installed on the LLNL ETA-II accelerator for testing.

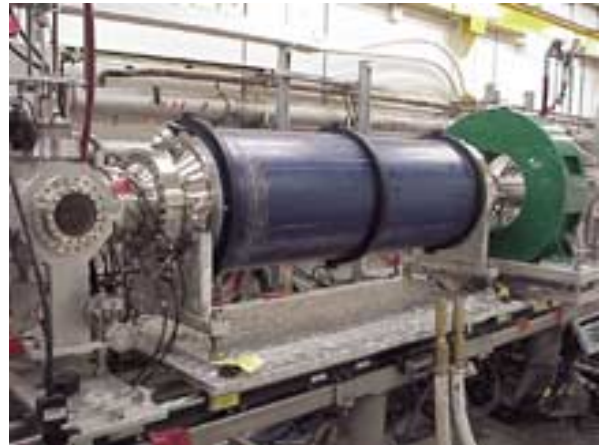


Fig. 7 The DARHT Kicker installed on ETA-II

The Kicker modulator is a solid-state inductive adder with a nominal output voltage of  $\pm 18$ -kV. Corrections for beam/Kicker interactions and the details of the power feed to the Kicker requires the ability to place fine modulation onto each Kicker pulse. In addition, micropulse width and spacing must be adjustable from the control room. Fig. 8 demonstrates the ability of the Kicker modulator to meet these needs. This is a measured 4-pulse output overlaid onto a typical, pre-programmed pulse train.

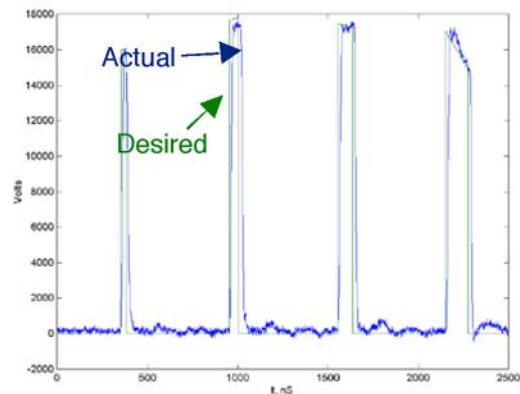


Fig. 8. Kicker pulser output demonstrating a 4-pulse train and the ability to generate arbitrary modulation to each micropulse.

#### 5. X-RAY CONVERSION TARGET

The initial 4-pulse target will consist of a low density ( $\sim 10\%$  normal density) tungsten foam target, about 1-cm in length, held within a tungsten cylinder that provides radial confinement of the target. Distributing the target over an extended distance delays the axial outflow of plasma and

permits the generation of four x-ray pulses over a period of 2- $\mu$ s. Typically the first pulse will convert some of the target, as well as surface contaminants, into a plasma. Subsequent pulses can be protected from backstreaming ions by placing a mechanical barrier upstream of the target assembly. This barrier foil is essentially transparent to the 20-MeV electron beam. Foil life can be ensured by proper tailoring of the beam size. Plasma lengths over 2- $\mu$ s (< 2 cm.) will not significantly disrupt the focal spot.

We have constructed a two-pulse x-ray conversion target test facility at the LLNL ETA-II accelerator. We have placed the 1-MeV, kiloamp "SNOWTRON" injector source immediately downstream of a target test cell on the ETA-II machine. SNOWTRON delivers a beam along the centerline of ETA-II, but fired into the target from the back side as ETA-II's beam strikes the target from the other side. The target is range thin leading to symmetric heating from the beam pulses. Therefore, beam entrance from the front or the back of the target is essentially the same. With this equipment, we can begin target disassembly by firing the SNOWTRON pulse, strike the expanding target with the ETA-II beam, and measure the x-ray spot size. We can also use one beam to probe the target density by generating x-rays from the expanding target and observing the x-ray conversion efficiency to measure the target hydrodynamic expansion.

Of critical importance is maintenance of a x-ray spot size that is  $\leq 2.1$ -mm for all four electron beam micropulses. Using the radially-confined foam target with an upstream barrier foil, we have demonstrated a stable ETA-II x-ray spot 500-ns after the SNOWTRON pulse has begun target disassembly. Fig. 9 shows images from an x-ray scintillator camera system demonstrating a stable spot with the barrier system. Without the foil barrier the

spot grows quickly to such a size that the resulting x-ray intensity is too low for any significant light output from the scintillator.

## 6. INITIAL OPERATIONS

Phase 2 prototype testing for accelerator components has been completed. Installation of the Injector is nearly complete and the vacuum system has achieved its design base pressure. RGA analysis indicates all specified partial pressures are within specification for cathode activation. After appropriate safety reviews, we will begin to operate the Injector Marx into the diode load to ensure that Marx installation has been successful and that the previous Marx test results can be reproduced at Los Alamos. Injector beam operation should begin by the end of the calendar year. During Injector commissioning, accelerator installation will continue from the high-energy end of the machine, working toward the injector. Beam will be transported through the accelerator by the end of calendar year 2002. After accelerator commissioning, beam will be directed through the Kicker and transport line to the x-ray conversion target. Following target commissioning, routine hydrodynamics testing will commence in 2004.

## 7. REFERENCES

- [1] Burns, M.J. et al, "DARHT Accelerators Update and Plans for Initial Operation", *IEEE 1999 Part. Accel. Conf.*, New York, NY, 1999
- [2] Holst, G.C., *Sampling, Aliasing, and Data Fidelity for Electronic Imaging Systems, Communications, and Data Acquisition*, SPIE JCD Publishing, 1998.
- [3] D. Simmons and C. Fortgang, "Using Multispectral Imaging to Measure Temperature Profiles and Emissivity of a Large Thermionic Dispenser Cathode", submitted to *Review of Scientific Instruments*
- [4] T.P. Hughes, "Design of Beam Cleanup Zone for DARHT-2", Mission Research Corp. Report MRC/ABQ-R-1958, Jan. 2000
- [5] Chen, Y.J.(Judy), et al, "Precision Fast Kickers For Kiloampere Electron Beams", *IEEE 1999 Part. Accel. Conf.*, New York, NY, 1991

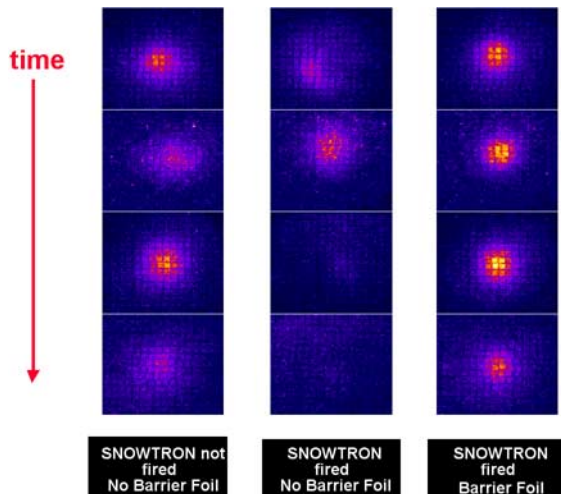


Fig. 9 ETA-II x-ray spot size images 500-ns after the x-ray conversion target is struck by the SNOWTRON beam. Without the barrier foil the x-ray spot is so large the x-ray intensity results in only a very low scintillator light output. With the barrier foil the x-ray spot is stable and intense.